Probing QCD spectral functions on the lattice

Harvey Meyer

From Euclidean spectral densities to real-time physics,
CERN, 13 March 2019

Cluster of Excellence

JOHANNES GUTENBERG UNIVERSITÄT MAINZ

European Research Council
Established by the European Commission

Outline

- Probing QCD spectral functions with the Backus-Gilbet method
- Vacuum spectral functions: numerical examples
- The pion quasiparticle in the low-temperature phase of QCD.

List of coauthors & references

- Bastian B. Brandt, Anthony Francis, Daniel Robaina, *Pion quasiparticle in the low-temperature phase of QCD*, 1506.05732 (PRD).
- Maxwell Hansen, HM, Daniel Robaina, *From deep inelastic scattering to heavy-flavor semileptonic decays: Total rates into multihadron final states from lattice QCD*, 1704.08993 (PRD).
- Maxwell Hansen, HM, Daniel Robaina, *Total decay and transition rates from LQCD*, DOI:10.1051/epjconf/201817513021.
- Tim Harris, HM, Daniel Robaina, *A variational method for spectral functions*, 1611.02499 (LAT2016).
- Bastian B. Brandt, Marco Cè, Anthony Francis, Tim Harris, HM, Aman Steinberg, *An estimate for the thermal photon rate from lattice QCD* , 1710.07050 (LAT2017)
- HM, *Euclidean correlators at imaginary spatial momentum and their relation to the thermal photon emission rate*, 1807.00781 (EPJA).

Photon production rate in the quark-gluon plasma: talk by Arianna Toniato.

Definitions

Euclidean-time vector correlators

$$G^{\mu\nu}(x_0, \boldsymbol{k}) = \int d^3x \, e^{-i\boldsymbol{k}\cdot\boldsymbol{x}} \Big\langle j^\mu(x) \, j^\nu(y) \Big\rangle, \qquad j^\mu = \sum_f Q_f \, \bar{\psi}_f \gamma^\mu \psi_f$$

- all diagonal components of $G^{\mu\nu}$ are positive; spectral representation:

$$G^{\mu\nu}(x_0, \boldsymbol{k}) \overset{\mu=\nu}{=} \int_0^\infty \frac{d\omega}{2\pi} \, \rho^{\mu\nu}(\omega, \boldsymbol{k}) \, \underbrace{\frac{\cosh[\omega(\beta/2 - x_0)]}{\sinh(\beta\omega/2)}}_{\overset{T \to 0}{\rightsquigarrow} e^{-\omega|x_0|}}.$$

- with appropriate subtractions, dispersive relation possible in momentum space, e.g.

$$\Delta\tilde{G}^{\mu\nu}(\omega_n, \boldsymbol{k}, T) \equiv \tilde{G}^{\mu\nu}(\omega_n, \boldsymbol{k}, T) - \tilde{G}^{\mu\nu}(\omega_n, \boldsymbol{k}, 0) = \int_0^\infty \frac{d\omega}{\pi} \omega \frac{\Delta\rho^{\mu\nu}(\omega, \boldsymbol{k}, T)}{\omega^2 + \omega_n^2}.$$

The Backus-Gilbert method (1/2)

$$\text{Linearity:} \qquad \sum_{i=1}^{n} c_i(\bar{\omega})\, G(t_i) = \int_0^\infty \frac{d\omega}{2\pi}\, \rho(\omega) \underbrace{\sum_{i=1}^{n} c_i(\bar{\omega})\, \frac{\cosh[\omega(\beta/2 - t_i)]}{\sinh[\omega\beta/2]}}_{\widehat{\delta}(\bar{\omega},\omega)}$$

- choose the coefficients $c_i(\bar{\omega})$ so that the 'resolution function' $\widehat{\delta}(\bar{\omega},\omega)$ is as narrowly peaked around a given frequency $\bar{\omega}$ as possible and normalized:

$$\int_0^\infty d\omega\; \widehat{\delta}(\bar{\omega},\omega) = 1$$

Idea behind the Backus-Gilbert method, used in Robaina et al. PRD 92 (2015) 094510.

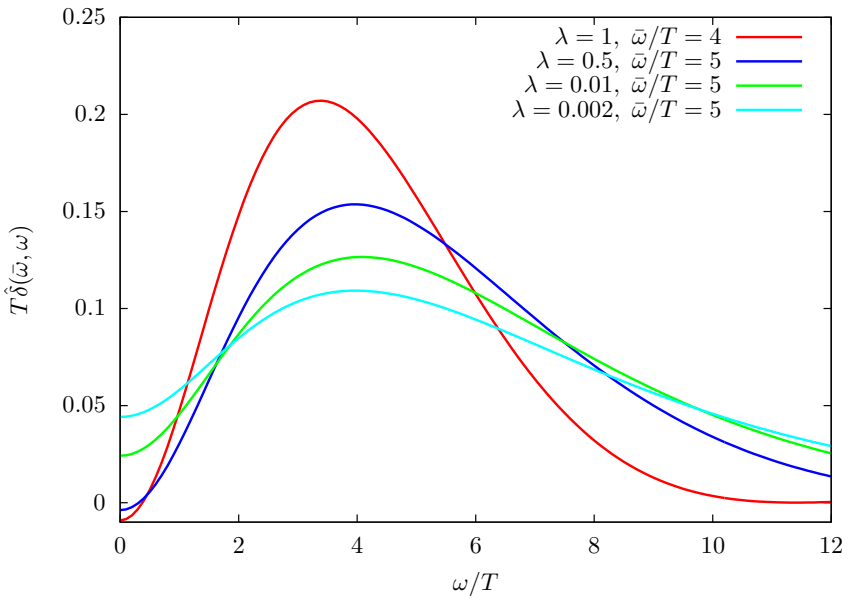

Resolution function at $\bar{\omega} = 4T$ for $N_t = 24$, $t_i/a = 5, \ldots 12$.

- Resolution only improves slowly with increasing n
- Large, sign-alternating coefficients $\Rightarrow$ need for ultra-precise input data.

Backus-Gilbert method (2/2)

Choose $f(\omega)$ such that $\frac{\rho(\omega)}{f(\omega)}$ is expected to be slowly varying:

$$G(t_i) = \int_0^\infty \frac{d\omega}{2\pi} \frac{\rho(\omega)}{f(\omega)} \left[f(\omega) \frac{\cosh[\omega(\beta/2 - t_i)]}{\sinh[\omega\beta/2]} \right] \quad \Rightarrow$$

Then one can obtain model-independently a smoothened/smeared version of the spectral function:

$$(S_f \rho)(\omega) \equiv f(\omega) \int_0^\infty d\omega' \; \delta_f(\omega, \omega') \; \rho(\omega') = f(\omega) \sum_{i=1}^{n} c_i(\omega) G(t_i).$$

If $\frac{\rho(\omega)}{f(\omega)}$ is constant, the BG method is exact. Further aspects:

- In practice: balance statistical uncertainty against resolution in frequency space with a Lagrange multiplier λ;
- for instance, request highest possible resolution around a given ω for a statistical precision of 5% or 10%.
- This is not a least-χ^2 method: one should not expect $\int_0^\infty \frac{d\omega}{2\pi} (S_f \rho)(\omega) \frac{\cosh[\omega(\beta/2-t)]}{\sinh[\omega\beta/2]}$ to give a good approximation to $G(t)$ in the sense of the χ^2.

Numerical tests at (virtually) $T = 0$

- $N_{\mathrm{f}} = 2$ QCD ensemble O7 generated within CLS
- 128×64^3, $a = 0.0483(4)$fm (1205.5380), $m_\pi = 269(3)$MeV
- $T = 32$MeV

At $T = 0$, $G(x_0) = \int_{\omega_{\mathrm{thr}}}^{\infty} d\omega \; e^{-\omega x_0} \rho(\omega)$: ω_{thr} is part of the prior knowledge.

Isovector correlators considered:

- $\int d^3x \, \langle V_i(x) V_i(0) \rangle$ (set $\omega_{\mathrm{thr}} = 2m_\pi$)
- $\int d^3x \, \langle A_i(x) A_i(0) \rangle$ (set $\omega_{\mathrm{thr}} = 3m_\pi$)
- $\int d^3x \, \langle V_i(x) V_i(0) - A_i(x) A_i(0) \rangle$ (set $\omega_{\mathrm{thr}} = 2m_\pi$)
- $\int d^3x \, \langle P(x) P(0) \rangle$ (set $\omega_{\mathrm{thr}} = 0$; or subtract pion contribution, and then set $\omega_{\mathrm{thr}} = 3m_\pi$)

Statistics: 490 configurations, 16 sources per configuration.

Study carried out by K. Zapp.

Examples of realistic resolution functions

$\omega_{\rm thr} = 0,\ f_0(\omega) = \tanh(\beta\omega/2);$

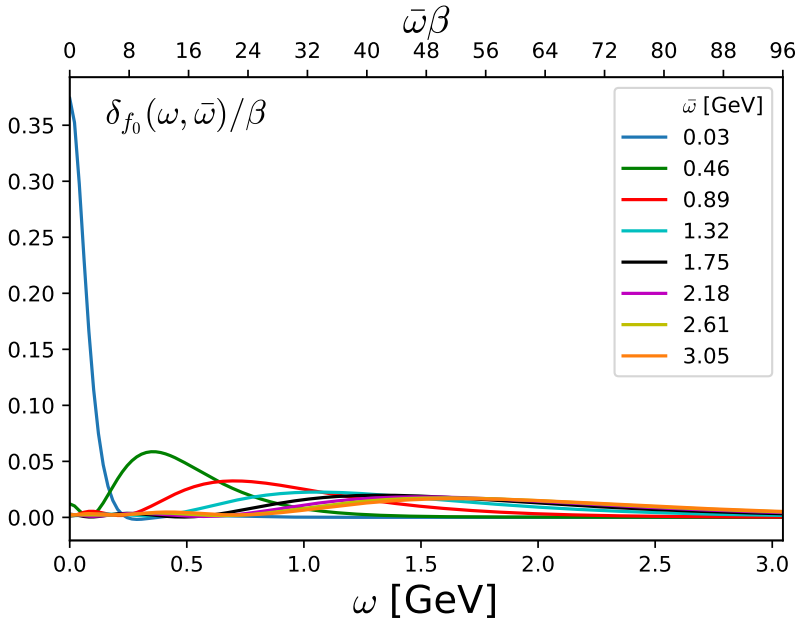

$\omega_{\rm thr} = 2m_\pi,\ f_1(\omega) = \dfrac{\omega^2}{\tanh(\beta\omega/2)}.$

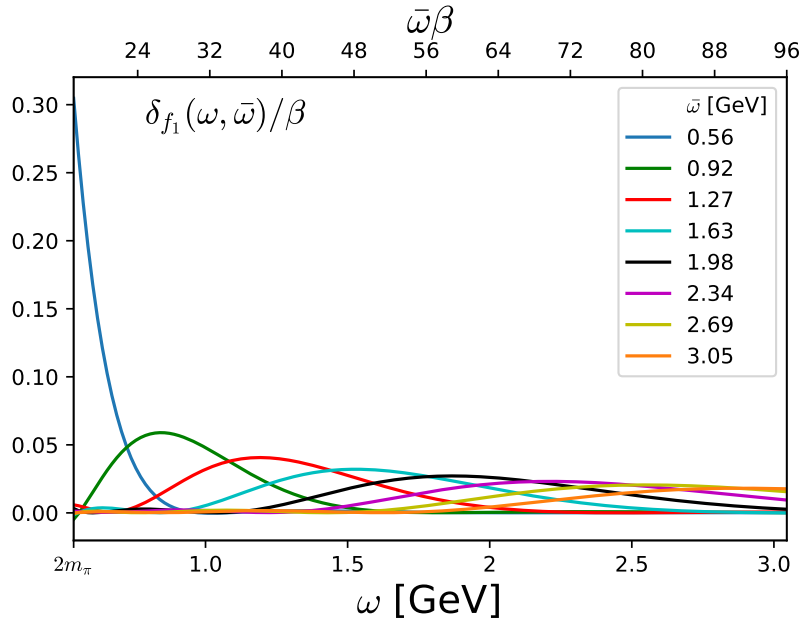

- the resolution deteriorates as one moves away from the threshold.

Free vacuum vector correlator in infinite volume

$$f_1(\omega) = \frac{\omega^2}{\tanh(\beta\omega/2)}$$

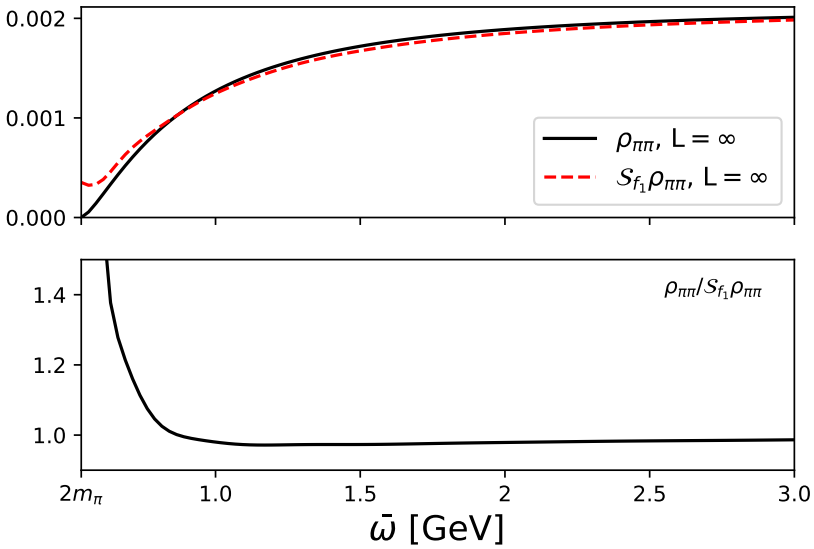

The phase-space factor $(1 - 4m_\pi^2/\omega^2)^{3/2}$ is recovered in a satifactory manner.

See Hansen et al. 1704.08993 for similar studies.

$$f_2(\omega) = \frac{\omega^2(1 - 4m_\pi^2/\omega^2)^{3/2}}{\tanh(\beta\omega/2)}$$

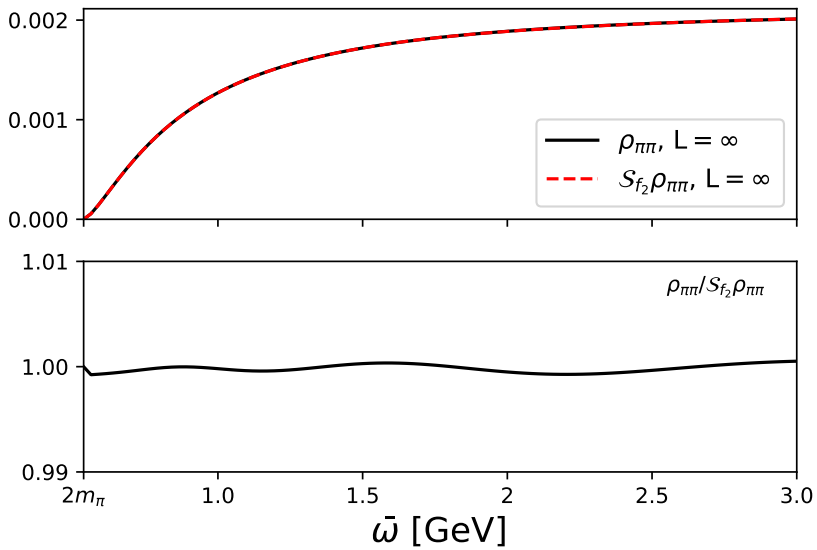

$(S_{f_2}\rho)(\omega) = \rho(\omega)$ in this case.

Free vacuum vector correlator in finite volume, $m_\pi L = 4.2$

$$f_1(\omega) = \frac{\omega^2}{\tanh(\beta\omega/2)}$$

$$f_2(\omega) = \frac{\omega^2(1-4m_\pi^2/\omega^2)^{3/2}}{\tanh(\beta\omega/2)}$$

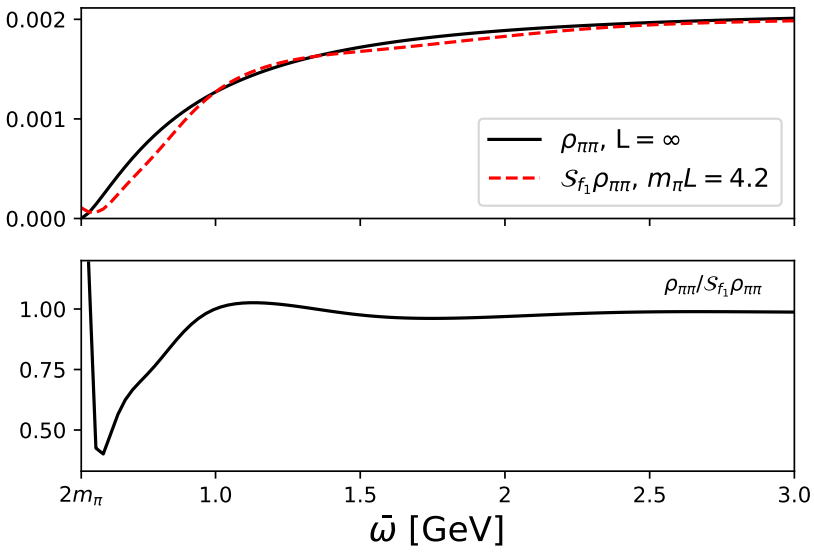

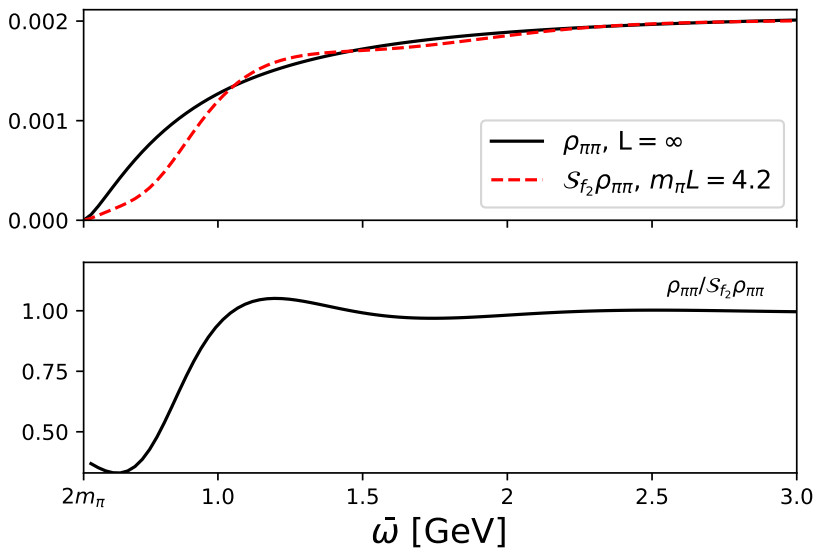

Applied to the free finite-volume correlator, including the phase-space factor is not necessarily beneficial.

Vacuum vector correlator: study with the Gounaris-Sakurai model

$$f_1(\omega) = \frac{\omega^2}{\tanh(\beta\omega/2)}$$

$$f_2(\omega) = \frac{\omega^2(1-4m_\pi^2/\omega^2)^{3/2}}{\tanh(\beta\omega/2)}$$

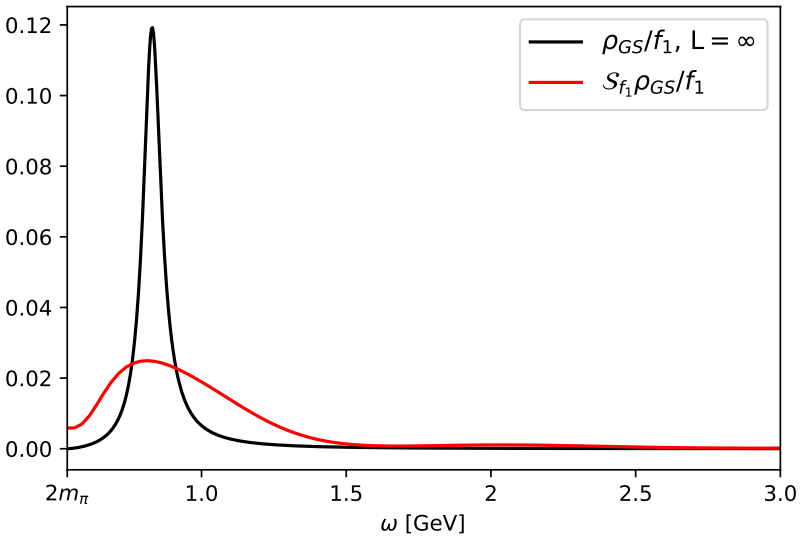

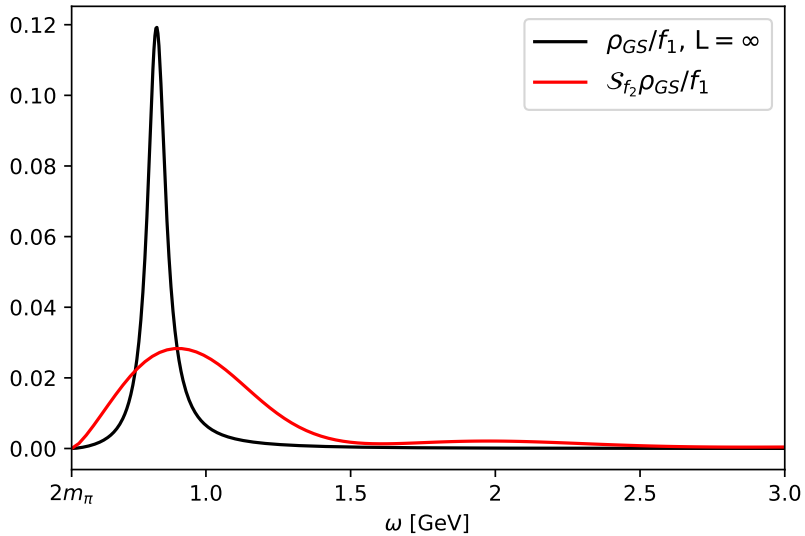

Black curve corresponds to $\frac{1}{48\pi^2}(1-4m_\pi^2/\omega^2)^{3/2}|F_{\rm GS}(\omega)|^2$,
with $F_{\rm GS}(\omega)$ the Gounaris-Sakurai parametrization of the pion form factor.

Finite-volume correlator

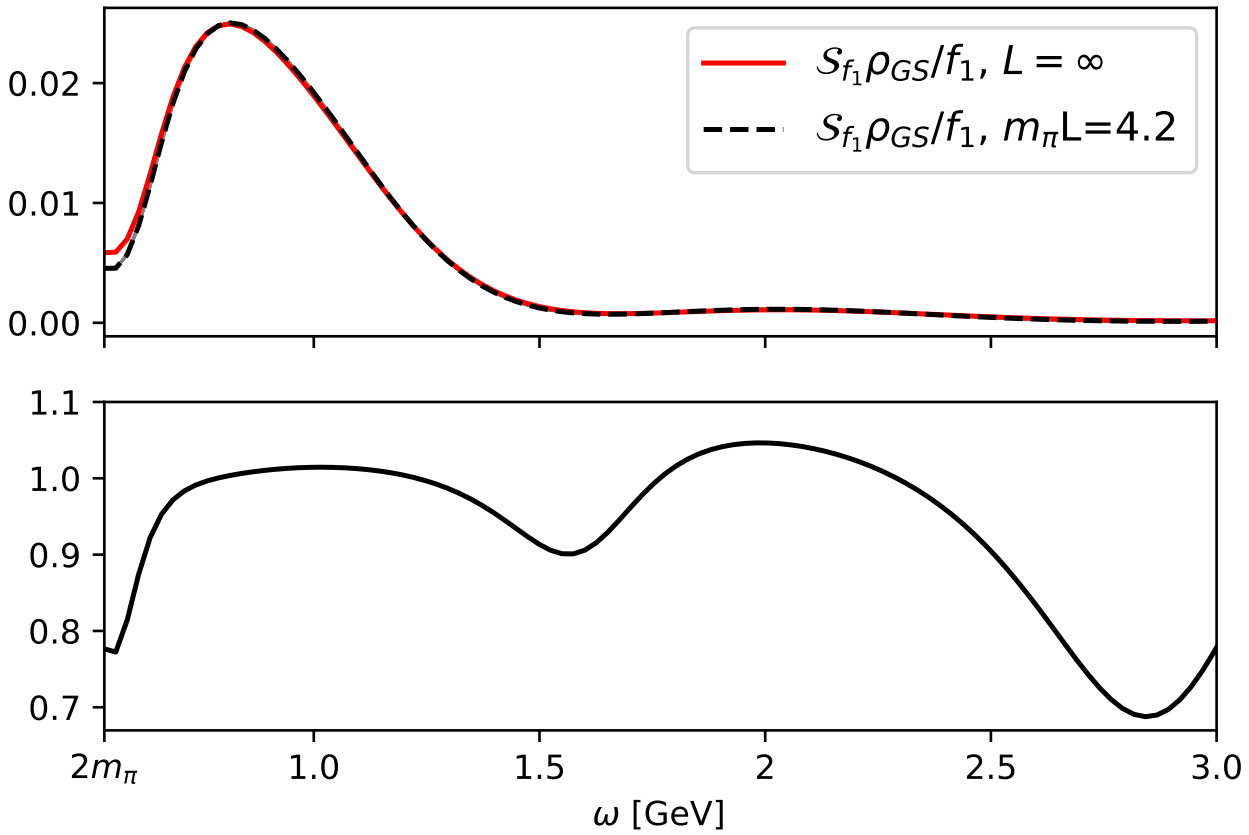

Smoothened version of $\frac{1}{48\pi^2}(1-4m_\pi^2/\omega^2)^{3/2}|F_{\rm GS}(\omega)|^2$.

Finite-volume correlator yields essentially the same smoothened spectral function: at present, we are limited by the resolution, not by finite-size effects.

Vacuum vector correlator: study with real lattice data (O7)

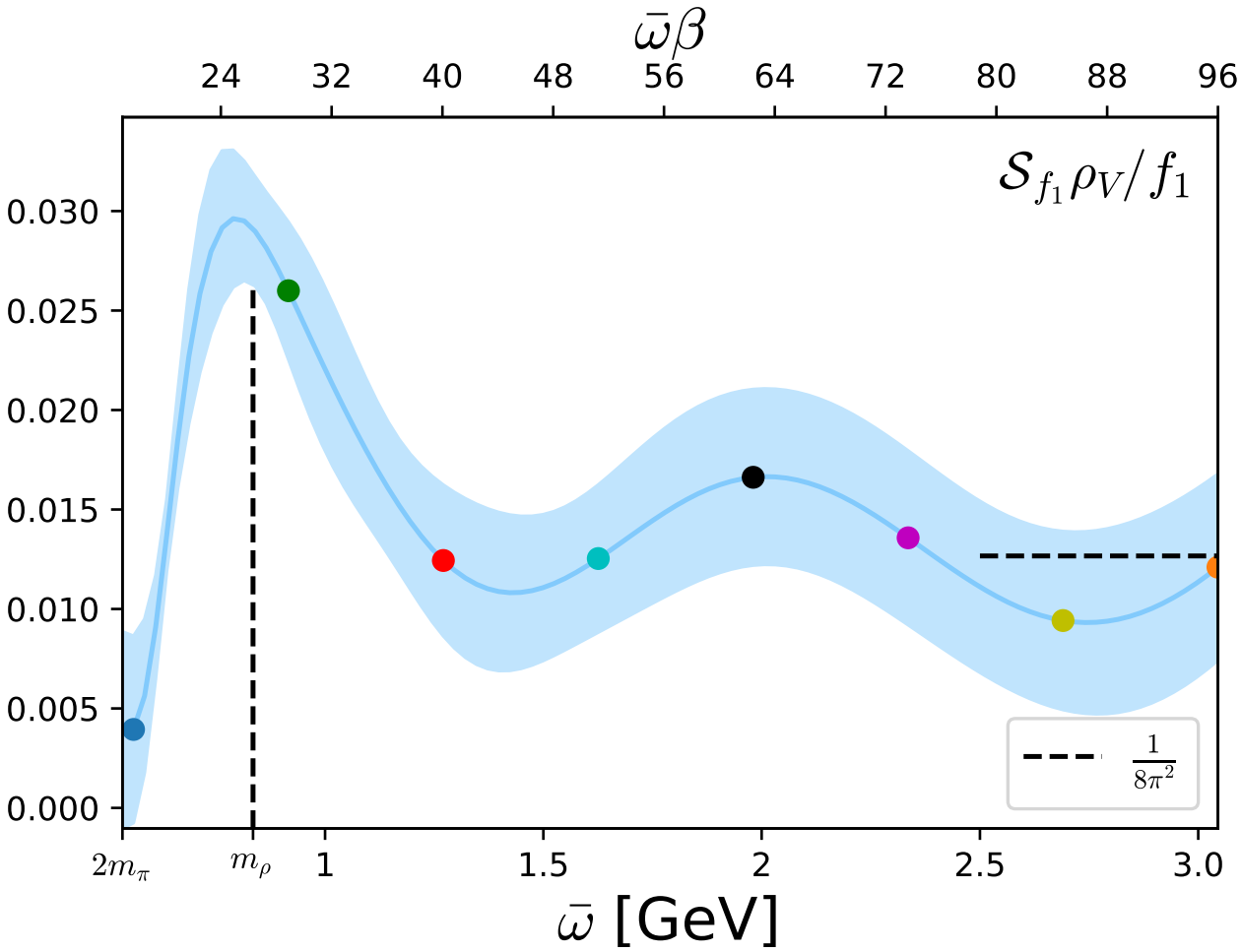

- Blue curve = smoothened version of $\frac{R_1(s)}{12\pi^2}$, where $R_1(s) = \frac{\sigma(e^+e^- \to (I{=}1) \text{ hadronic state})}{4\pi\alpha^2/(3s)}$.
- $f_1(\omega) = \omega^2/\tanh(\beta\omega/2)$.

The (isovector) R-ratio: lattice (O7) vs. pheno

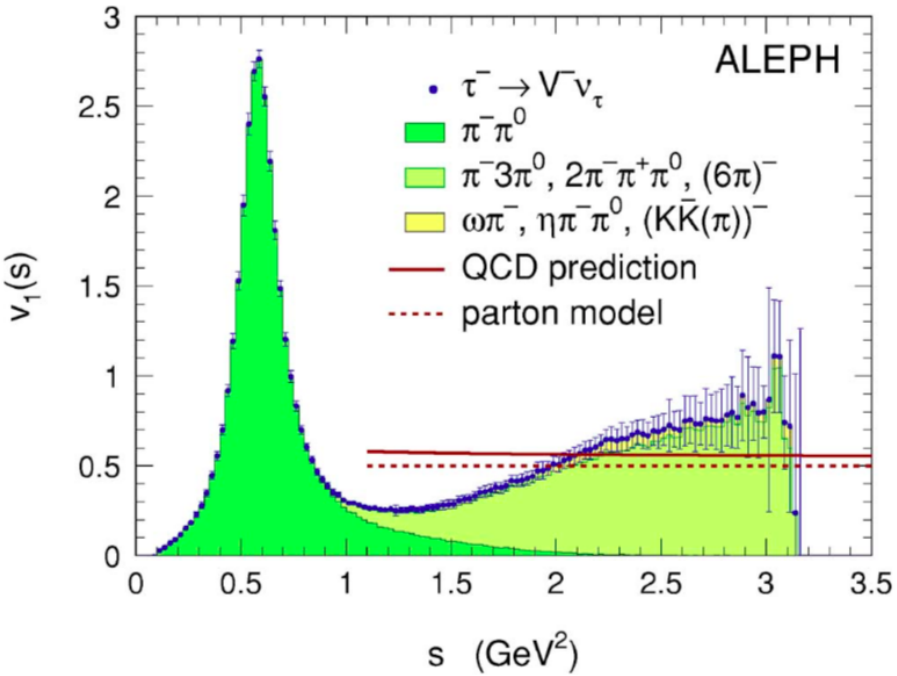

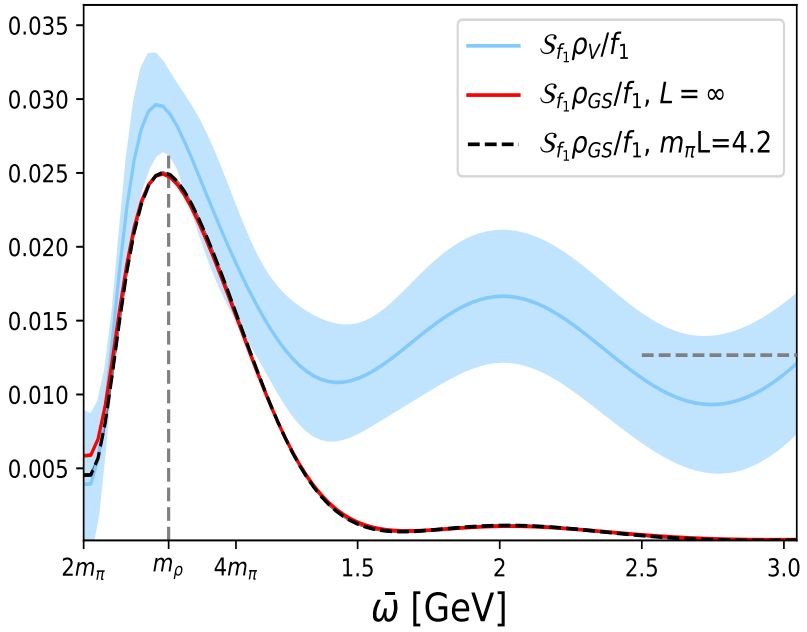

$v_1(s) = \frac{1}{3} R_1(s)$ up to isospin breaking corr.

From Davier, Höcker, Zhang

DOI:10.1103/RevModPhys.78.1043

Blue curve = smoothened version of $\frac{R_1(\bar{\omega}^2)}{12\pi^2}$

$$R_1(s) \equiv \frac{\sigma(e^+e^- \to \ (I=1) \text{ hadronic state})}{4\pi\alpha^2/(3s)}$$

The $\langle VV - AA \rangle$ correlator: comparison to phenomenology

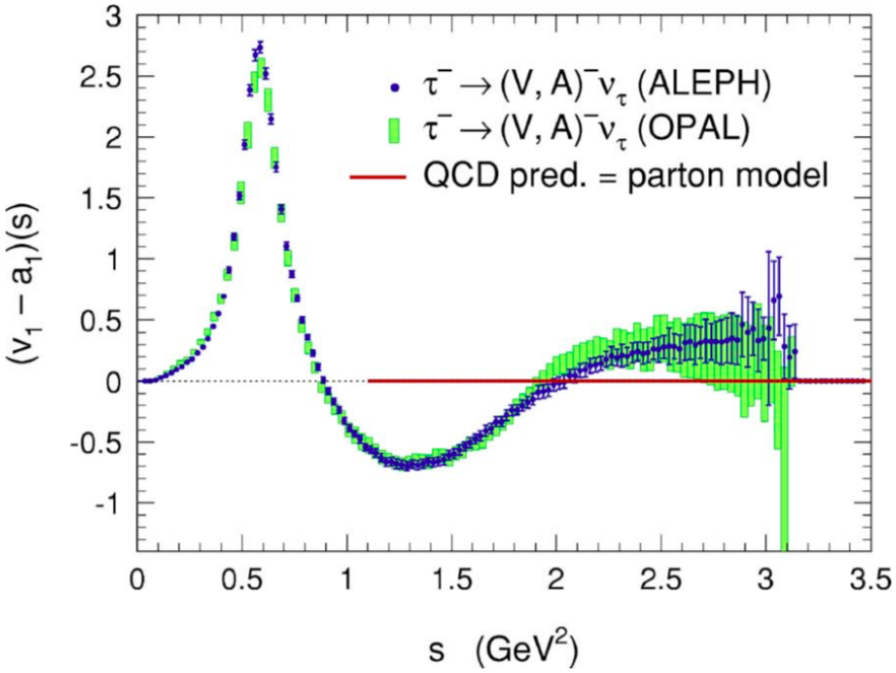

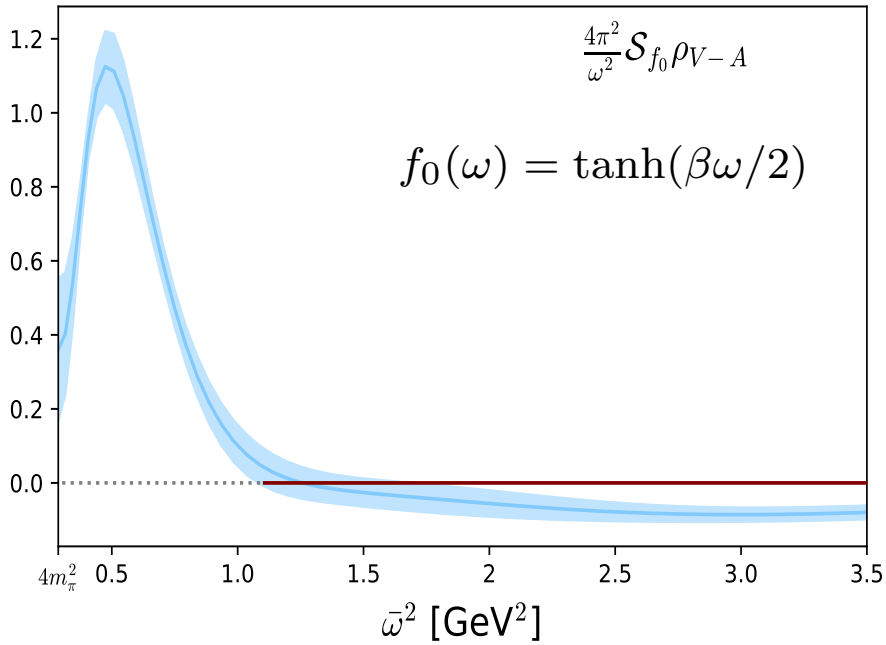

From Davier, Höcker, Zhang
DOI:10.1103/RevModPhys.78.1043

Blue curve = smoothened version of $v_1(s) - a_1(s)$.

The negative contribution of the a_1 meson is spread over a wide frequency interval in $(S_{f_0} \rho_{V-A})$.

The pion channels: $\langle PP \rangle$

$$f_1(\omega) = \frac{\omega^2}{\tanh(\beta\omega/2)}$$

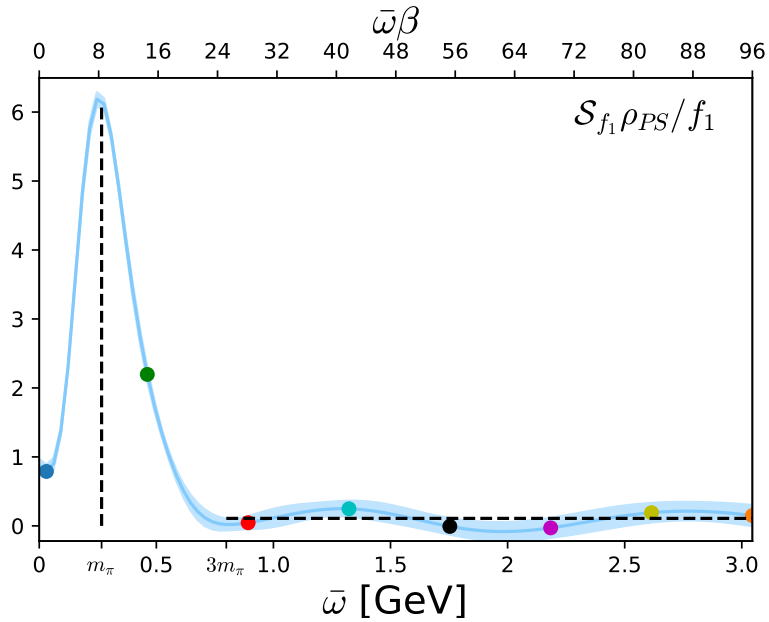

Applying BG to the $\langle PP \rangle$ correlator.

The pion delta-function gets 'smeared'.

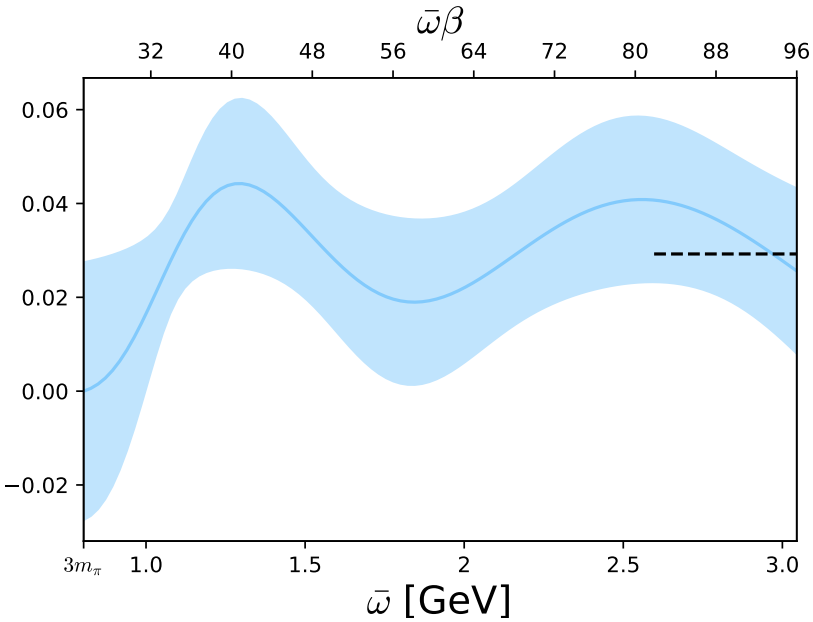

Applying BG after subtracting the pion contribution, obtained as usual by fitting the correlator at large Euclidean time.

Prospects for improvement

How the resolution improves with the nb. of data if precision is very high:

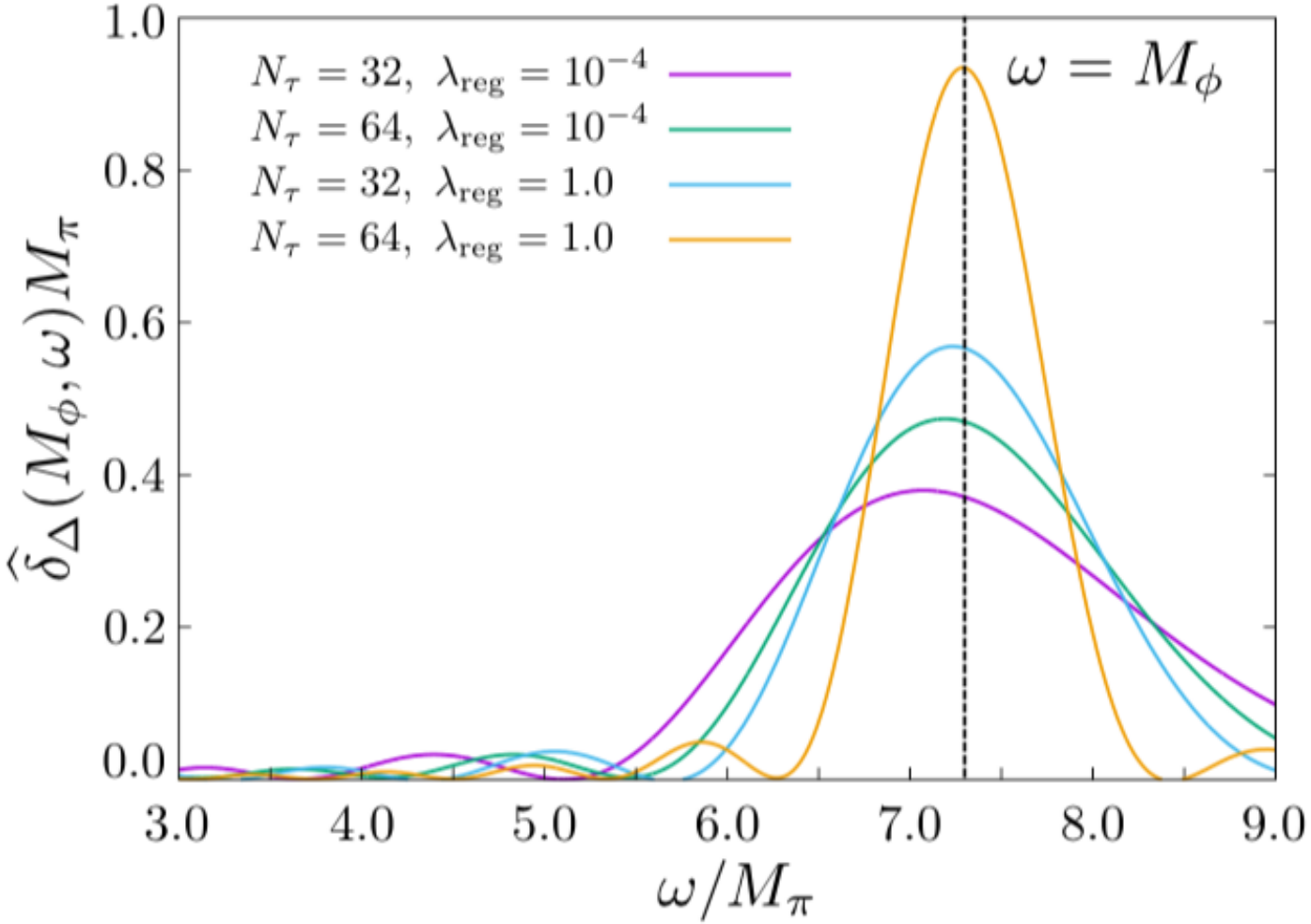

Other option: subtract the contribution of $\pi\pi$ states for $\omega < 4m_\pi$ using Lellouch-Lüscher type relations, apply BG on the rest.

Fig. by D. Robaina from 1704.08993.

Aspects of the low-T phase of $N_{\mathrm{f}} = 2$ QCD

The pion quasiparticle in the low-temperature phase

- Chiral symmetry is spontaneously broken for $T < T_c$: $-\langle\bar{\psi}\psi\rangle > 0$.
- Goldstone theorem $\Rightarrow$ a divergent spatial correlation length exists in the limit $m \to 0$.
- somewhat less obvious: a massless real-time excitation exists: the pion quasiparticle.

Static screening correlator:

$$\int dx_1\, dx_2 \int_0^\beta dx_0\, \langle A_3(x) A_3(0)\rangle = f_\pi^2 m_\pi^2 \cdot \frac{e^{-m_\pi |x_3|}}{2m_\pi} + \ldots .$$

Time-dependent correlator:

$$\int d^3x\, e^{i\boldsymbol{p}\cdot\boldsymbol{x}}\, \langle A_0(x) A_0(0)\rangle = f_\pi^2 (m_\pi^2 + \boldsymbol{p}^2) \cdot \frac{\cosh[\omega_{\boldsymbol{p}}(\beta/2 - x_0)]}{2\omega_{\boldsymbol{p}} \sinh[\omega_{\boldsymbol{p}}\beta/2]} + \ldots ,$$

Quasiparticle dispersion relation:

$$\omega_{\boldsymbol{p}} = u\sqrt{m_\pi^2 + \boldsymbol{p}^2} + \ldots$$

[Son and Stephanov, PRD 66, 076011 (2002); D. Robaina et al. 1406.5602; 1506.05732.]

Study at $T \simeq 170\,\mathrm{MeV}$

- $(N_\mathrm{f} = 2)$ 24×64^3 (O7) lattice; $m_\pi(T=0) \simeq 270\,\mathrm{MeV}$; $T_c \approx 210\,\mathrm{MeV}$;
- we find

$$\left[\frac{\langle\bar\psi\psi\rangle_T}{\langle\bar\psi\psi\rangle_0}\right]_{\mathrm{GMOR}} \equiv \frac{(f_\pi^2 m_\pi^2)_T}{(f_\pi^2 m_\pi^2)_0} = 0.76(4)$$

  i.e. a substantial reduction in the chiral condensate.

- Pion properties:

$$T = 0: \qquad \text{pion mass} = 267(2)\,\mathrm{MeV}$$
$$\swarrow \qquad\qquad \searrow$$
$$T = 169\mathrm{MeV}: \quad \text{quasiparticle mass} = 223(4)\mathrm{MeV} \qquad \text{screening mass} = 303(4)\mathrm{MeV}.$$

- The 'velocity' $u = \omega_{\mathbf{0}}/m_\pi = 0.74(1)$ is quite far from unity.

Robaina et al. 1506.05732.

How was it done? Extracting the pion quasiparticle mass

Important point:

pion dominates Euclidean two-point function of A_0 and of P at $x_0 = \beta/2$:

$$\text{PCAC relation}: \quad \frac{\partial^2}{\partial x_0^2} \int d^3x \langle A_0(x) A_0(0) \rangle = -4m_q^2 \int d^3x \langle P(x) P(0) \rangle$$

$$\Rightarrow \qquad \omega_{\mathbf{0}} = \left[-4m_q^2 \frac{\int d^3x \langle P(x) P(0) \rangle}{\int d^3x \langle A_0(x) A_0(0) \rangle} \right]^{1/2} .$$

Testing the prediction for the residue of the pion pole

Another option to determine $\omega_{\mathbf{0}}$: solve

$$\frac{1}{f_\pi^2 m_\pi^2} \int d^3x \, \langle A_0(x) A_0(0) \rangle = \frac{\cosh[\omega_{\mathbf{0}}(\beta/2 - x_0)]}{2\omega_{\mathbf{0}} \sinh[\omega_{\mathbf{0}}\beta/2]} + \ldots$$

for $\omega_{\mathbf{0}}$.

If the chiral effective theory is consistent, the same result should come out as on the previous slide.

NB. Here we only rely on the pion dominating the A_0 correlator, not the P correlator; on the other hand, we rely on the residue being correctly predicted by the chiral effective theory.

Within two standard deviations, the same result is indeed obtained.

1406.5602; 1506.05732.

Lighter pion mass, $T \simeq 150\,\mathrm{MeV}$

Very similar results obtained on a 20×64^3 (G8) lattice at smaller pion mass, $m_\pi(T=0) = 185\,\mathrm{MeV}$:

- $\omega_{\mathbf{0}} = 155(5)\,\mathrm{MeV}$
- $u = 0.78(3)$.
- Also, ChEFT predictions consistent with lattice data up to $|\boldsymbol{p}| \approx 300\,\mathrm{MeV}$.
- At finite $\boldsymbol{p}$, we have used either the BG method or an explicit fit ansatz for the spectral function.

K. Zapp et al. 1801.00298.

Test of the Gell-Mann–Oakes–Renner relation at $T \simeq 150\,\mathrm{MeV}$

16×48^3, $m_\pi(T=0) \approx 305$ and 217 MeV

Current algebra prediction: $(\omega_0^2 f_\pi^{t\,2})_T = (m_\pi^2 f_\pi^2)_T = -m_q \langle \bar{\psi}\psi \rangle_T$

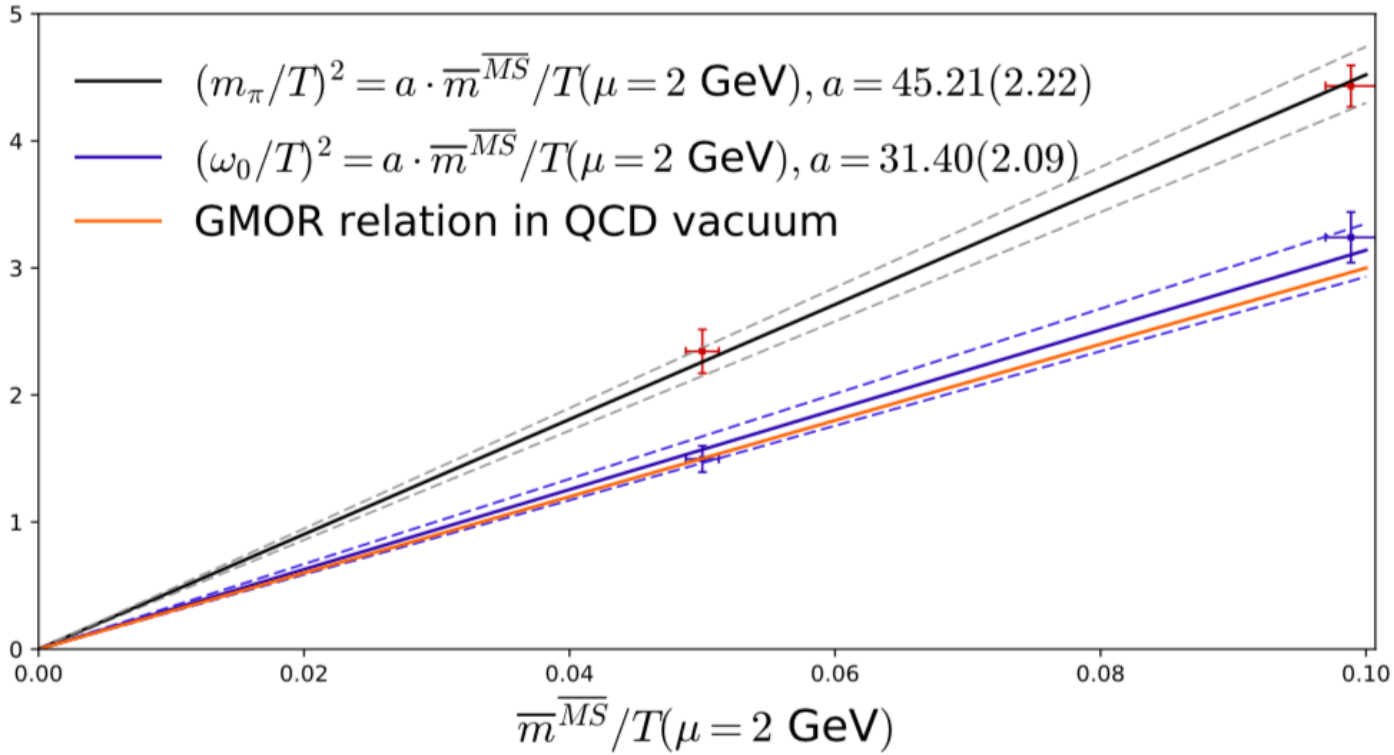

Both the pion screening mass and the pion quasiparticle mass follow the GMOR relation at $m_\pi \lesssim 300\,\mathrm{MeV}$ at $T \approx 150\,\mathrm{MeV}$.

K. Zapp et al. 1801.00298; $T = 0$ result from Engel et al. 1406.4987.

The $\langle V_i V_i - A_i A_i \rangle$ correlator at $p = 0$

Recall the vacuum result (O7, $m_\pi = 269\,\mathrm{MeV}$):

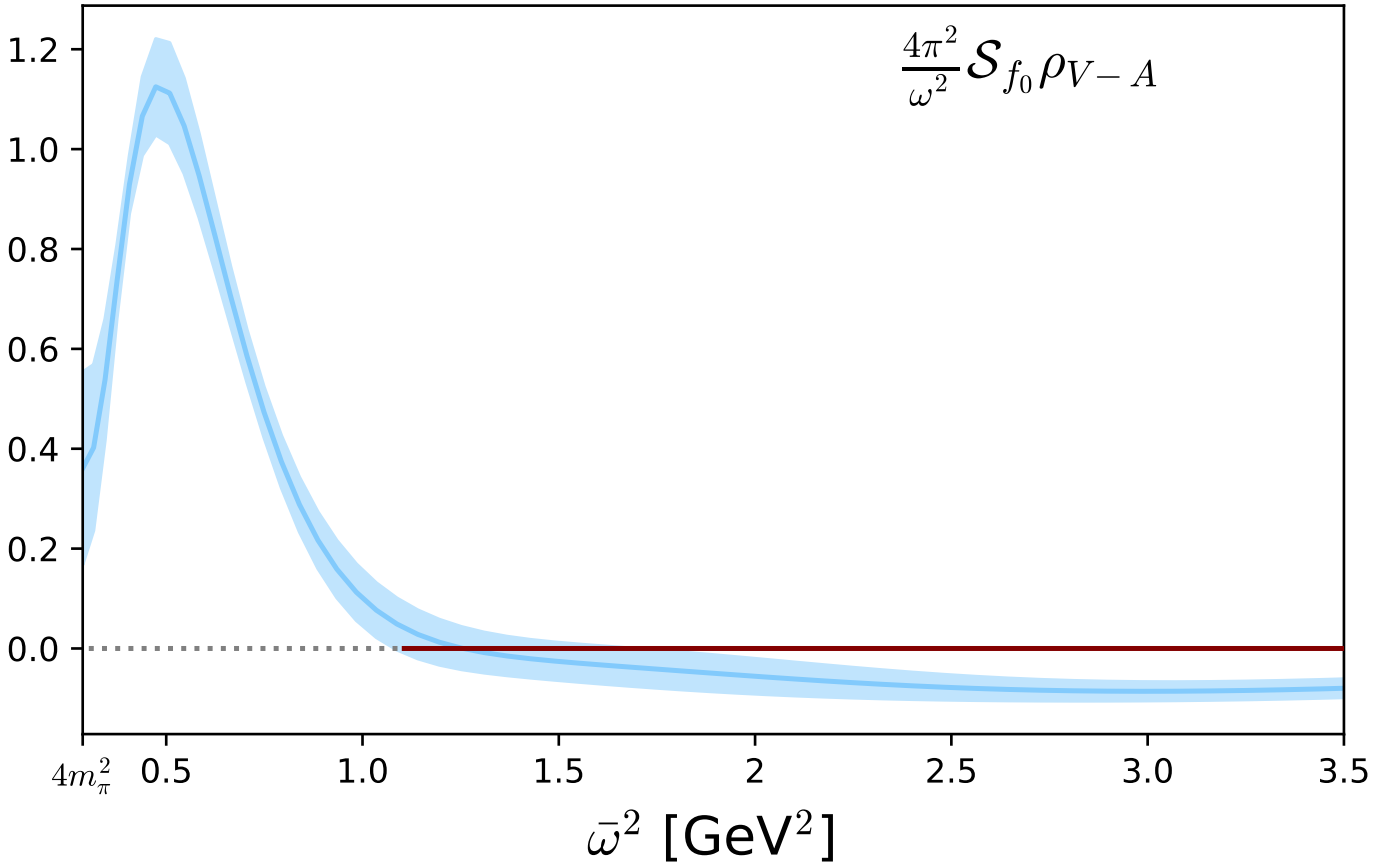

- this difference of spectral functions is an order parameter for chiral symmetry
- expect vanishing difference at $T > T_c$, up to small $\mathrm{O}(m_q^2)$ effects.

ChPT prediction for $\langle V_i V_i - A_i A_i \rangle$ at low temperature

In the chiral limit and at low $|\boldsymbol{p}|, T \ll f_\pi$:

$$\rho_V(\omega, \boldsymbol{p}, T) - \rho_A(\omega, \boldsymbol{p}, T) = (1 - 2\epsilon)[\rho_V(\omega, \boldsymbol{p}, 0) - \rho_A(\omega, \boldsymbol{p}, 0)], \quad \epsilon = \frac{T^2}{6 f_\pi^2}.$$

This can be tested on the lattice: if this relation holds literally, the ratio of the thermal to the 'reconstructed' correlator should be constant and equal to $(1 - 2\epsilon)$.

'Reconstructed' correlator = the Euclidean correlator that would be obtained at finite T if the spectral function remained the same as at $T = 0$:

$$G^{\mathrm{rec}}_{V-A}(x_0, \boldsymbol{p}, T) = \sum_{n \in \mathbb{Z}} G_{V-A}(x_0 + \frac{n}{T}, \boldsymbol{p}, 0).$$

Dey, Eletsky, Ioffe, PLB 252, 620 (1990); K. Zapp et al 1801.00298.

Lattice results on $\langle V_i V_i - A_i A_i \rangle$ at $T = 170\,\mathrm{MeV}$ 24×64^3 (07)

Reconstructed correlator

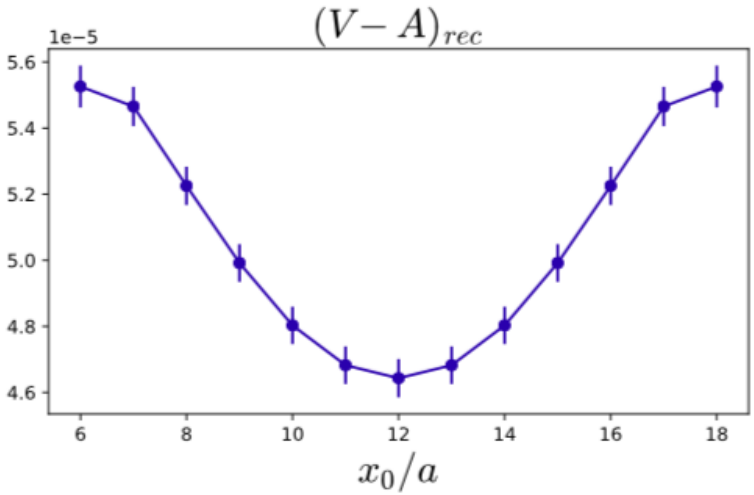

Thermal correlator

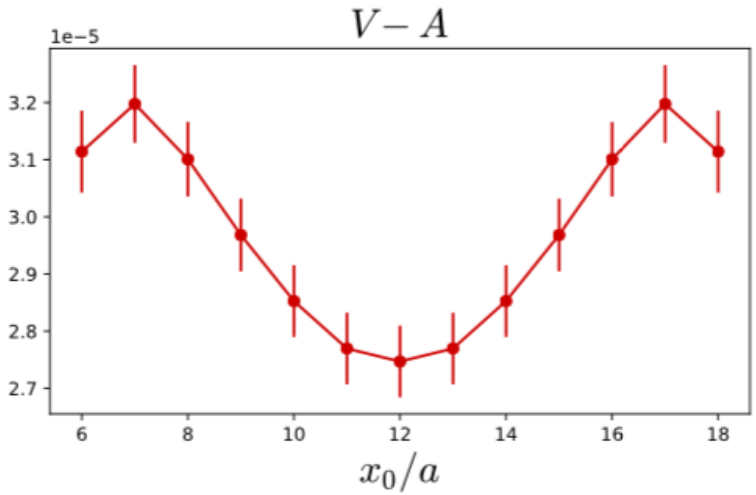

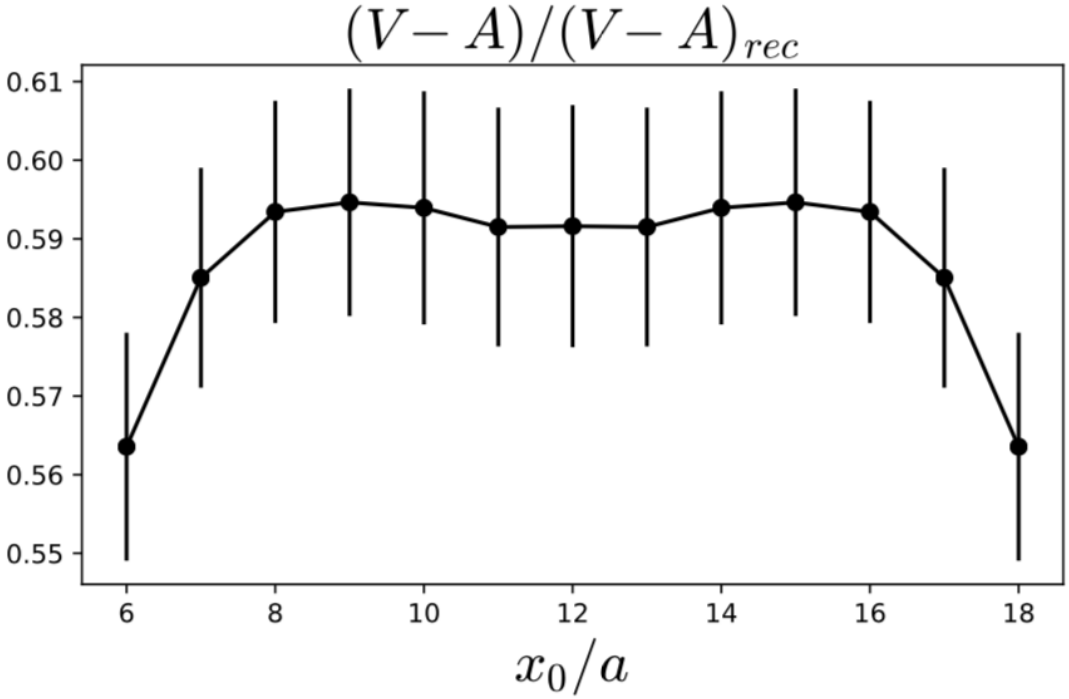

Lattice results on $\langle V_i V_i - A_i A_i \rangle$ at $T = 170\,\mathrm{MeV}$ 24×64^3 (07)

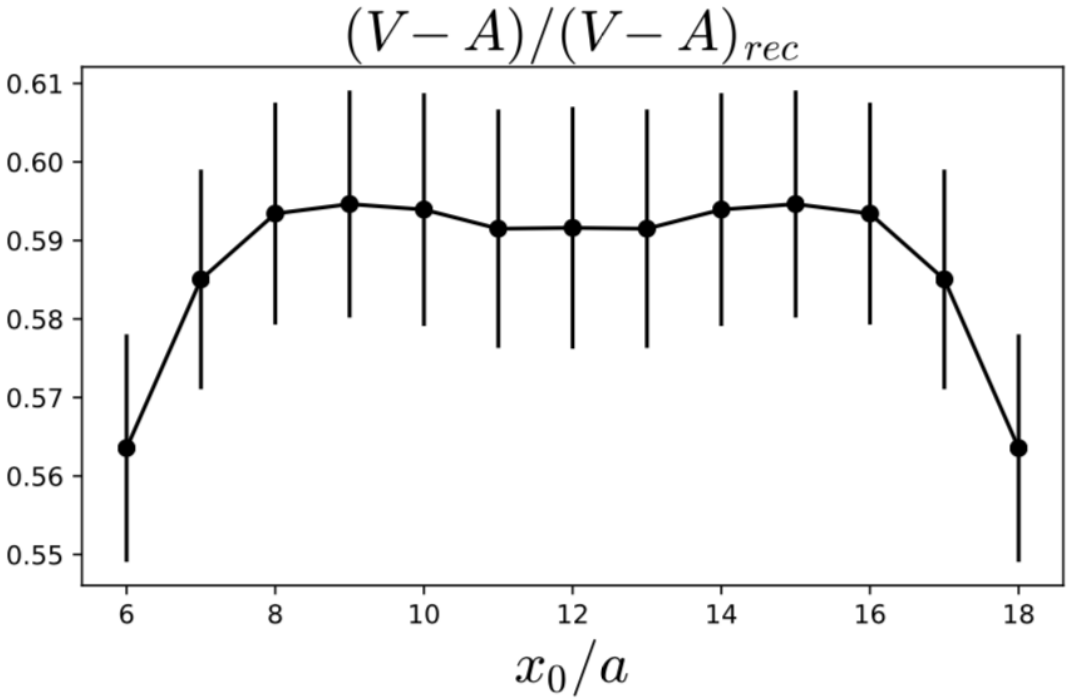

- the ratio is indeed quite flat;
- reduction by a factor 0.60 at the largest accessible Euclidean times;
- chiral symmetry restoration is quite advanced in this observable; also seen in screening vector and axial-vector masses;
- at $x_0 \leq \beta/4$, cutoff effects need to be studied carefully.

Brandt et al 1608.06882; 1801.00298

Conclusion

- The Backus-Gilbert method allows for a model-independent probing of QCD spectral functions from lattice correlators, albeit at rather low frequency resolution.
- The method is robust against finite-size effects.
- It is systematically improvable, at the cost of having very high accuracy correlators.

Summarizing our findings at $T = 170\,\text{MeV}$ compared to $T = 0$, for $m_\pi(T=0) \simeq 270\,\text{MeV}$:

$$\Big(\underbrace{\omega_{\mathbf{0}}^2}_{\text{reduced}} \quad \underbrace{f_\pi^{t\,2}}_{\text{unchanged}}\Big)_T = \Big(\underbrace{m_\pi^2}_{\text{increased}} \quad \underbrace{f_\pi^2}_{\text{much reduced}}\Big)_T = -m_q \quad \underbrace{\langle\bar\psi\psi\rangle_T}_{\text{reduced by } \sim 3/4}$$

The thermal width of the pion, however, presently remains numerically inaccessible. . .

Backup slides

A dispersion relation for a Euclidean correlator at zero virtuality

- Let $\sigma(\omega) \equiv \rho_T(\omega, |\boldsymbol{k}| = \omega)$ be the relevant spectral function proportional to the photon emission rate;
- let $H_E(\omega_n) \equiv G_E(\omega_n, k = i\omega_n)$ the momentum-space Euclidean correlator with Matsubara frequency ω_n and *imaginary* spatial momentum $k = i\omega_n$;
- once-subtracted dispersion relation: ($\sigma(\omega) \sim \omega^{1/2}$ at weak coupling)

$$H_E(\omega_n) - H_E(\omega_r) = \int_0^\infty \frac{d\omega}{\pi}\, \omega\, \sigma(\omega) \Big[\frac{1}{\omega^2 + \omega_n^2} - \frac{1}{\omega^2 + \omega_r^2} \Big].$$

Representation through non-static screening masses

$$\tilde{G}_E(\omega_r, x_3) = -2\int_0^\beta dx_0\, e^{i\omega_r x_0}\int dx_1 dx_2\, \langle J_1(x)J_1(0)\rangle = \sum_n |A_n^{(r)}|^2 e^{-E_n^{(r)}|x_3|}$$

$$\Rightarrow \underbrace{H_E(\omega_r)}_{=\mathrm{O}(g^2)} \equiv \int_{-\infty}^{\infty} dx_3\, \tilde{G}_E(\omega_r, x_3)\, e^{\omega_r x_3} = 2\omega_r^2 \sum_{n=0}^{\infty} \underbrace{|A_n|^2}_{=\mathrm{O}(g^4)} \underbrace{\frac{1}{E_n^{(r)}\,(E_n^{(r)2} - \omega_r^2)}}_{=\mathrm{O}(g^{-2})}.$$

This helps explain the connection observed in [Brandt et al, 1404.2404] between non-static screening masses and the LPM-resummation contributions to the photon emission rate [Aurenche et al, hep-ph/0211036].

In lattice regularization, Lorentz symmetry is absent $\Rightarrow H_E(\omega_r)$ does not vanish in vacuum as it does in the continuum. Explicitly subtracting the *in vacuo* $H_E(\omega_r)$ from the thermal $H_E(\omega_r)$ may be necessary.

Sketch of the (standard) derivation of the dispersion relation

$G_R(\omega,k) = i(\delta_{il} - \frac{k_i k_l}{k^2}) \int d^4x\, e^{i\mathcal{K}\cdot x}\theta(x^0) \left\langle [\mathrm{j}^i(x), \mathrm{j}^l(0)] \right\rangle$. But

$$[j^\mu(x), j^\nu(0)] = 0 \quad \text{for} \quad x^2 < 0,$$

$\Rightarrow$ the retarded correlator $H_R(\omega) \equiv G_R(\omega, k=\omega)$ at lightlike momentum is analytic for $\mathrm{Im}\,(\omega) > 0$. Similarly, the advanced correlator $H_A(\omega)$ is analytic for $\mathrm{Im}\,(\omega) < 0$.

Define the function $H(\omega) = \begin{cases} H_R(\omega) & \mathrm{Im}\,(\omega) > 0 \\ H_A(\omega) & \mathrm{Im}\,(\omega) < 0 \end{cases}$.
It is analytic everywhere, except for a discontinuity on the real axis:

$$H(\omega + i\epsilon) - H(\omega - i\epsilon) = H_R(\omega) - H_A(\omega) = i\sigma(\omega),$$

Write a Cauchy contour-integral representation (using two half-circles) of $H(\omega)$ just above the real axis, where it coincides with $H_R(\omega)$:

$$H_R(\omega) = H_R(\omega_r) + \int_{-\infty}^{\infty} \frac{d\omega'}{2\pi}\, \sigma(\omega') \Big[\frac{1}{\omega' - \omega - i\epsilon} - \frac{1}{\omega' - \omega_r - i\epsilon} \Big].$$

The dispersion relation for the Euclidean correlator follows from the observation $G_E(\omega_n, k^2) = G_R(i\omega_n, k^2), \qquad n > 0.$